RECONSTRUCTION OF 3D TOOTH IMAGES

S. Buchaillard[1], *S.H. Ong*[1,2], *Y. Payan*[3], *K.W.C. Foong*[4]

[1]Department of Electrical and Computer Engineering, National University of Singapore, Singapore
[2]Division of Bioengineering, National University of Singapore, Singapore
[3]TIMC/IMAG laboratory, UMR CNRS 5525, Université Joseph Fourier, France
[4]Department of Preventive Dentistry, National University of Singapore, Singapore

ABSTRACT

We describe a novel approach to obtain a good estimate of the complete 3D representation of a tooth given only the crown. The technique is based on the use of a statistical model derived from 3D images of teeth constructed by microtomography. The root is constructed by matching the respective crowns of the two models, defining the optimal registration, and optimizing the statistical model parameters. This method allows us to generate the root efficiently due to the small number of parameters to adjust, and requires little or no interaction from the user. The resultant 3D model is smooth and provides a good approximation of the root shape.

1. INTRODUCTION

Accurate knowledge of the 3D shape of teeth and the positions of the roots is very important in many maxillofacial surgical applications, endodontic procedures, and treatment simulations. For example, a dental implant can be inserted into the jawbone when a tooth is missing to act as a substitute for the root. Using the mirror image of the corresponding tooth on the other side of the jaw to define a 3D representation of the missing tooth could result in an implant of better quality. Among image acquisition modalities, computer tomography (CT) is the most efficient way of generating 3D objects. However, CT imaging of dental patients is not always available and is radiologically invasive. Therefore, to overcome this problem, alternative methods have been developed to approximate the root shape.

Enciso et al.[1] have suggested a 3D reconstruction based on 2D radiographs, resulting in a "best fit" patient-specific 3D geometric polygonal mesh of a tooth using thin-plate splines. However, this method does not consider the possible shape variations of a given tooth and uses only 2D image data.

In this paper, we describe a novel approach for obtaining the shape of a tooth using only 3D crown information and without the use of X-rays, CT or MRI. Various methods may be employed to acquire highly accurate crown models, e.g., direct imaging with an intra-oral camera (OraScanner from OraMetrix GmbH) or laser scanning of a plaster cast of the patient's dentition. Once the three-dimensional crown model has been built, we still need a method to reconstruct the root. Section 2 presents the construction of a statistical shape model whose variations describe how the shape of a particular tooth can vary. Section 3 describes the registration problem and explains how the statistical model can be fitted to the patient's crown to produce a good estimate of the shape and size of the reconstructed tooth. Finally, in section 4, experimental results are presented to demonstrate the capabilities of this approach.

2. CONSTRUCTION OF A STATISTICAL MODEL

2.1. Data Collection

Twenty-two 3D tooth samples of the second upper-right premolar were imaged with a SkyScan-1076 microCT scanner at a resolution of 35 μm. The contour of each tooth was manually defined on each CT slice and the resulting surface model was decimated (giving a new resolution of 105 μm) before further processing. Each tooth was then matched with a generic tooth model using the procedure described by Szeliski and Lavallée [2], resulting in a collection of $N = 22$ 3D training shapes of the same tooth. This approach requires aligning manually each training tooth with a generic one that is represented by an M-point 3D triangular mesh. Non-rigid registration [2] using free-form deformation [3] and splines is then performed to deform the generic model to match each training tooth. Each resulting example is finally represented by a vector

$$\mathbf{m} = (x_0, y_0, z_0, \ldots, x_{M-1}, y_{M-1}, z_{M-1})$$

Fig. 1(a) shows the generic tooth model used for matching. An example of the 3D tooth models reconstructed from microtomography is seen in Fig. 1(b). Fig. 1(c) shows the same tooth after non-rigid registration.

0-7803-8554-3/04/$20.00 ©2004 IEEE.

(a) (b) (c)

Fig. 1. Generic model and elastic registration onto a tooth exemplar. (a) Generic model. (b) Tooth exemplar reconstructed from microtomography. (c) Generic model matched onto the exemplar.

2.2. Construction of a Point Distribution Model

A statistical shape model, the point distribution model (PDM) [4], can be used to describe the average shape and shape variations of a set of sample models. The mean shape $\bar{\mathbf{m}}$ is defined using

$$\bar{\mathbf{m}} = \frac{1}{N} \sum_{i=0}^{N-1} \mathbf{m}_i \tag{1}$$

The modes of variation, symbolizing the ways in which the points tend to move together, can be found by computing the eigenvectors $\mathbf{e}_i$ of the covariance matrix $\mathbf{R}_{ac}$:

$$\mathbf{R}_{ac} = \frac{1}{N-1} \sum_{i=0}^{N-1} (\mathbf{m}_i - \bar{\mathbf{m}})(\mathbf{m}_i - \bar{\mathbf{m}})^T \tag{2}$$

Given the high resolution of the 3D models used, a direct estimate of the eigenvectors of R_{ac} is not feasible. Instead of working in the variable (tooth points) space $R^{3\times M}$ (dimension $3 \times M$), the eigenvectors are defined in training sample space R^N (dimension $N < 3 \times M$). Simple mathematical considerations [5] give us an immediate correspondence between the eigenvectors and eigenvalues in these two spaces. The eigenvalues in $R^{3\times M}$ and R^N are identical, and if $(\lambda_\alpha, \mathbf{u}_\alpha)$ are associated variables (eigenvector, associated eigenvalue) in $R^{3\times M}$, then $(\lambda_\alpha, \mathbf{v}_\alpha)$ are the corresponding associated variables (eigenvector, associated eigenvalue) in $R^{3\times N}$ where

$$\mathbf{v}_\alpha = \frac{1}{\sqrt{\lambda_\alpha}} \mathbf{X}\mathbf{u}_\alpha$$

and the rows of the $N \times 3M$ matrix $\mathbf{X}$ correspond to the tooth data points.

The proportion of the total variance explained by each vector is equal to the corresponding eigenvalues. Consequently, the eigenvectors $\mathbf{e}_i$ associated with the maximum eigenvalues λ_i correspond to the major deformation modes. Fig. 2 shows the cumulative percentage of variability given the number of components. Seven components can explain 95% of the variability, while thirteen components explain more than 99% of the variability between the different samples.

Any shape belonging to the training set can be approximated as a sum of the mean model and a linear combination of the first pc modes, i.e.,

$$\mathbf{m} = \bar{\mathbf{m}} + \sum_{i=0}^{pc-1} \omega_i \mathbf{e}_i \tag{3}$$

where ω_i are the weights associated with the eigenvectors $\mathbf{e}_i$. By constraining every ω_i such that $-\lambda_i \leq \omega_i \leq \lambda_i$ we can limit the amount of deviation from the mean model.

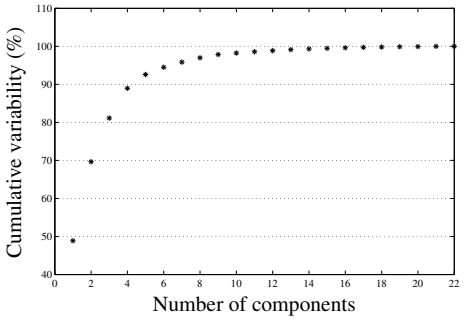

Fig. 2. Cumulative percentage of variability given the number of components.

2.3. 3D Mesh Model

The mean model consists of an unorganized cloud of points. In order to obtain a mesh boundary representation of the patient's tooth after reconstruction, a 3D reconstruction is performed using a marching cube algorithm [6] after extraction of the isosurface.

3. TOOTH RECONSTRUCTION

Once the statistical model has been defined, the patient's tooth shape is computed from the optimal rigid and elastic transformations of the mean model following Fleute et al. [7]. We aim to match the patient's crown with the corresponding region of our statistical model by determining the contribution of the different modes of the statistical model. The crown shape variations with respect to the mean model are then used to infer the root shape.

3.1. Initial Registration

In order to reconstruct the target tooth, an intermediate step can be included between between principal component analysis (PCA) (Section 2.2) and the final deformation. The iterative closest point (ICP) algorithm [8] can be used to perform the best possible alignment between the two models. This step is implemented with manual rigid registration and, if necessary, scaling. Although not mandatory, it can greatly

decrease the running time of the reconstruction and improve the final results.

3.2. Non-Rigid Deformation of the Statistical Model

The optimum parameters can be computed through the minimization of a merit function to measure the goodness-of-fit. The merit function used here (Equation 4) is the simple mean-squared distance (the Euclidean distance) between the crowns of the two volumes:

$$E(\mathbf{p}) = \sum_{i=0}^{M_c-1} \min(\|\mathbf{d}_j - \mathbf{m}_i\|^2)_{1\leq j\leq K} \quad (4)$$

$$\text{with } \mathbf{m} = \mathbf{R}(\bar{\mathbf{m}} + \sum_{l=0}^{N_{pc}-1} \omega_l \mathbf{e}_l) + \mathbf{T} \quad (5)$$

where $\mathbf{p}$ is a vector representing the different parameters to adjust, M_c the number of crown points of the PDM, K the number of points of the target tooth, $\mathbf{d}$ the vector representing the target (dimension $3 \times K$), $\mathbf{T}$ a translation vector, $\mathbf{R}$ a rotation matrix, and $\mathbf{e}_l$ the principal components obtained in part 2.2 (pc corresponds to the number of principal components selected).

We need to estimate the six components that define the rigid-body transformation between the two volumes (three parameters each for $\mathbf{T}$ and $\mathbf{R}$) as well as the optimum weights for the N_{pc} principal components, i.e., we have to solve an optimization problem having only $6 + N_{pc}$ parameters.

The optimization of $E(\mathbf{p})$ was performed using the Levenberg-Marquardt algorithm [9]. To compute the minimum distances, two different options were tested, with and without the use of a pre-computed distance map.

Computing the minimum distances is the most computationally expensive part of the minimization. In the first case, distances are approximated using an octree-splines distance map [2]. The two volumes (target and deformable models) are enclosed in a bounding box and a classical octree decomposition is realized based on the points of the patient's tooth. For each corner of the terminal octants, the minimum distance to the patient's tooth is computed and stored. Given a new point P, determining the minimum distance only requires that we find the octant the point belongs to and realizing a trilinear interpolation over the 8 corners of this octant. This method allows us to get a good approximation of the required distances. As for the partial derivatives with respect to every component, they can be computed by Ridder's method of polynomial extrapolation.

The second method uses kd-trees [10] that can be built in $\mathbf{O}(M \log M)$. A kd-tree is a binary tree used to represent data of dimension d (here $d = 3$). Each node of the binary tree represents a subset of the data record and a partitioning of that subset. The particular structure of a kd-tree makes it very easy to compute the required distances. This second method requires the construction of a new kd-tree after each iteration of the Levenberg-Marquardt algorithm. We can access the true distances and a closed-form expression for the gradient of $E(\mathbf{p})$ becomes available.

4. RESULTS

Two types of tests were performed to check the validity of the method described in this paper, the first using extracted teeth and the second patient data.

4.1. Leave-one-out Test

A leave-one-out test was realized using the 22 specimens for the two approaches described (with or without a distance map). Distances between the original specimens T_i and their reconstructed shape TR_i were estimated using the Hausdorff distance (HD) [11]. Table 1 summarizes the results obtained without pre-computed distance map and Figure 3 represents an example of reconstruction in the general case.

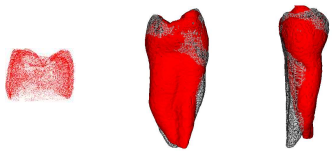

(a) (b) (c)

Fig. 3. (a) Crown information used for the reconstruction. (b) and (c) show the mesial and buccal views of the original tooth T and its reconstructed shape TR. The 3D mesh represents TR and the surface T.

	HD (mm)			HD (% teeth height)		
	Max	Mean	RMS	Max	Mean	RMS
Minimum	0.96	0.11	0.16	5.07	0.56	0.84
Maximum	5.30	0.51	0.86	28.19	2.56	4.59
Mean	2.42	0.29	0.49	12.44	1.50	2.50
Variance	0.80	0.01	0.03	22.27	0.20	0.72

Table 1. Leave-one-test results: reconstruction based on crown information, without pre-computed distance map ($N_{pc} = 7$).

For all the teeth of the test set, the reconstruction process lead to a perfect match between the crowns of TR_i and T_i. For the majority of the reconstructions, the method gave a very good approximation of the teeth height and width. Only one particular tooth in the training set lead to results far from those expected. Indeed, the reconstruction being based on a statistical representation, outliers will lead to erroneous results. For this particular specimen, the correlation usually observed between the height and width of a tooth, and the size of the crown (e.g., shape or width) was not respected and consequently produced a reconstructed model much larger than the original one.

4.2. Test using patient data

A second test was then realized using real data. A study model was digitized using a laser scanner Cyberware Rapid 3D Digitizer Model 3030R-HIREZ. The upper right second premolar was extracted using Kondo *et al.* 's method of segmentation [12] (Fig. 4a) and the 3D shape of the tooth determined (Fig. 4b). Despite the significant loss of information introduced by the segmentation, the reconstruction resulted in an excellent match between the original crown and those of the tooth computed.

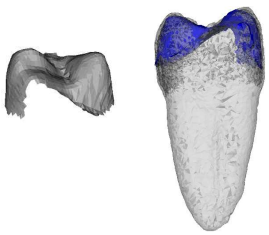

(a) (b)

Fig. 4. Process of fitting a tooth on a dental cast. (a) Crown of the tooth after segmentation. (b) Tooth after reconstruction (grey surface) and original crown (blue surface).

5. CONCLUSION

The method described in this paper proved to be effective to reconstruct a tooth given only crown information. Though it was realized using a particular kind of tooth, it could easily be extended to all single-rooted teeth. Furthermore, generating a new PDM per tooth is not absolutely necessary: mirror teeth can be reconstructed using the same training set, since the mirror PDM could be created using the mirror view of the mean shape and those of the different modes. Teeth whose shapes differ only in size (e.g., first and second premolar) could also use the same database (simple scaling of the mean shape and different modes of the PDM). To conclude, this method presents two major advantages: it exploits the entire prior information available for a given tooth and it requires little or no interaction from the user.

6. REFERENCES

[1] R. Enciso et al., "3D tooth shape from radiographs using thin-plate splines," in *MMVR11 NextMed: HealthHorizon, Proc. of the 11th Annual Medicine Meets Virtual Reality*, Jan. 2003, pp. 62–64.

[2] R. Szeliski and S. Lavallée, "Matching 3D anatomical surfaces with non-rigid deformations using octree-splines," *IJCV*, vol. 18, no. 2, pp. 171–186, 1996.

[3] T. W. Sederberg and S. R. Parry, "Free-form deformation of solid geometric models," *SIGGRAPH*, vol. 20, no. 4, pp. 151–160, 1986.

[4] T.F. Cootes et al., "Training models of shape from sets of examples," in *Proc. of the British Machine Vision Conference*, 1992.

[5] L. Lebart et al., *Statistique Exploratoire Multidimensionelle*, Dunod, third edition, 2000.

[6] W. Lorensen and H. Cline, "Marching cubes: A high resolution 3-D surface construction algorithm," *Computer Graphics*, vol. 21, pp. 163–169, 1987.

[7] M. Fleute et al., "Incorporating a statistically based shape model into a system for computer-assisted anterior cruciate ligament surgery," *Medical Image Analysis*, vol. 3, no. 3, pp. 209–222, 1999.

[8] P. J. Besl and N. D. McKay, "A method for registration of 3-D shapes," *IEEE Trans. on PAMI*, vol. 14, no. 2, pp. 239–256, Feb. 1992.

[9] W. H. Press et al., *Numerical Recipes in C++*, Cambridge University Press, second edition, 1992.

[10] A.W. Moore, *Efficient Memory-based Learning for Robot Control*, Ph.D. thesis, University of Cambridge, 1991, Tech. Rep. 209.

[11] N. Aspert et al., "Mesh: Measuring errors beween surfaces using the Hausdorff distance," in *Proceedings of the IEEE International Conference in Multimedia and Expo*, Aug. 2002, vol. 1, pp. 705–708, `http://mesh.epfl.ch`.

[12] T. Kondo et al., "Tooth segmentation of dental study models using range images," *IEEE Trans. Med. Imag.*, vol. 23, no. 3, pp. 350–362, Mar. 2004.